Horton et al., http://www.jcb.org/cgi/content/full/jcb.201508080/DC1

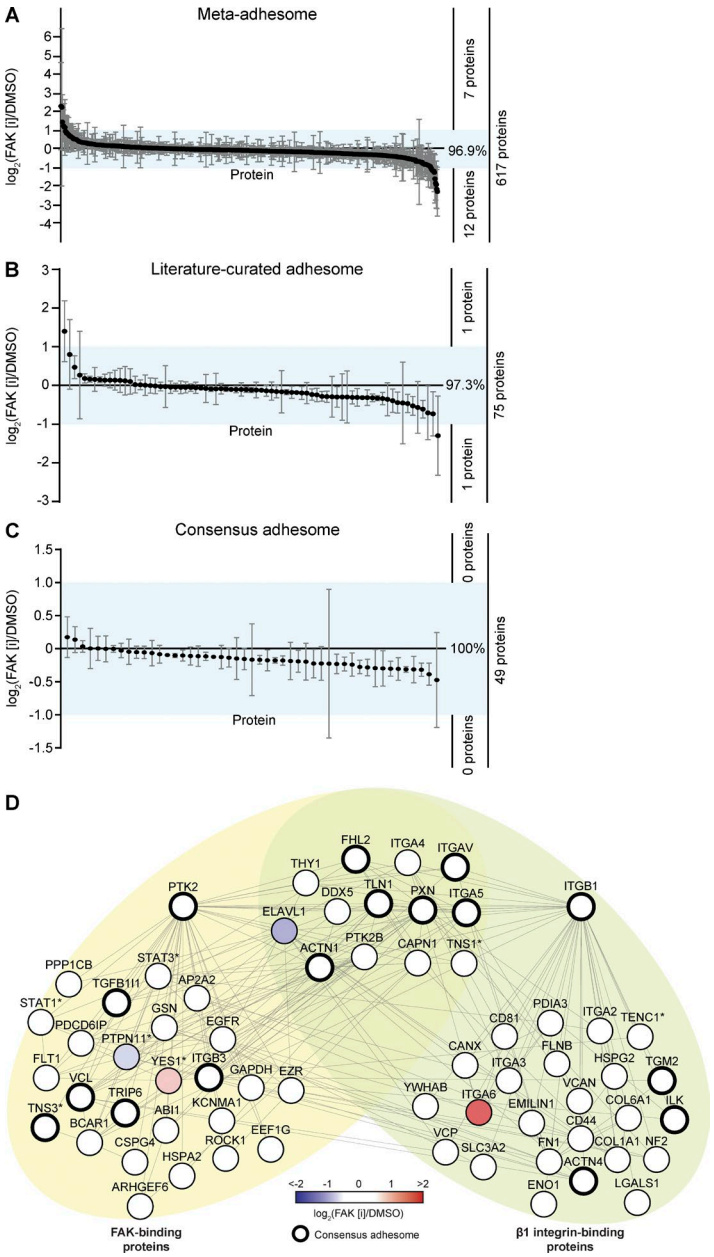

Figure S1. **MS-based proteomic analysis of IACs isolated from cells treated with DMSO or FAK [i].** HFF cells spread on FN for 1 h were treated with DMSO or 3 µM FAK [i] for 1 h. IACs were isolated by a combination of cross-linking, cell lysis, and high-pressure water wash and isolated IACs were analyzed by MS. Ratios of normalized intensity values (log_2(FAK [i]/DMSO)) were calculated for each protein in each replicate experiment. Graphs show mean ± SEM, $n = 3$. Blue shading corresponds to twofold or less change between conditions and the percentage of proteins within twofold change is indicated. (A) A graph of meta-adhesome (Horton et al., 2015) proteins identified by MS. Of the 617/2412 (25%) meta-adhesome proteins identified, seven proteins increased and 12 proteins decreased upon FAK inhibition by at least twofold. (B) A graph of literature-curated adhesome (Winograd-Katz et al., 2014) proteins identified by MS. Of the 75/232 (32%) literature-curated adhesome proteins identified, one protein increased and one protein decreased upon FAK inhibition by at least twofold. (C) A graph of consensus adhesome (Horton et al., 2015) proteins identified by MS. Of the 49/60 (82%) consensus adhesome proteins identified, no proteins increased or decreased upon FAK inhibition by at least 1.4-fold. (D) Protein–protein interaction network model of proteins identified by MS that are known to interact with FAK (PTK2) and/or β1 integrin (ITGB1). Identified proteins were mapped onto a human protein–protein interaction network. Proteins are indicated by colored circles and interactions are indicated by gray lines. Nodes are colored according to the mean fold change between FAK [i] and DMSO conditions (Table S2). Proteins that are members of the consensus integrin adhesome (Horton et al., 2015) are indicated by thick black node border and proteins reported to contain a SH2 domain in InterPro (Mitchell et al., 2015) are indicated by an asterisk. Proteins are labeled by gene name for clarity.

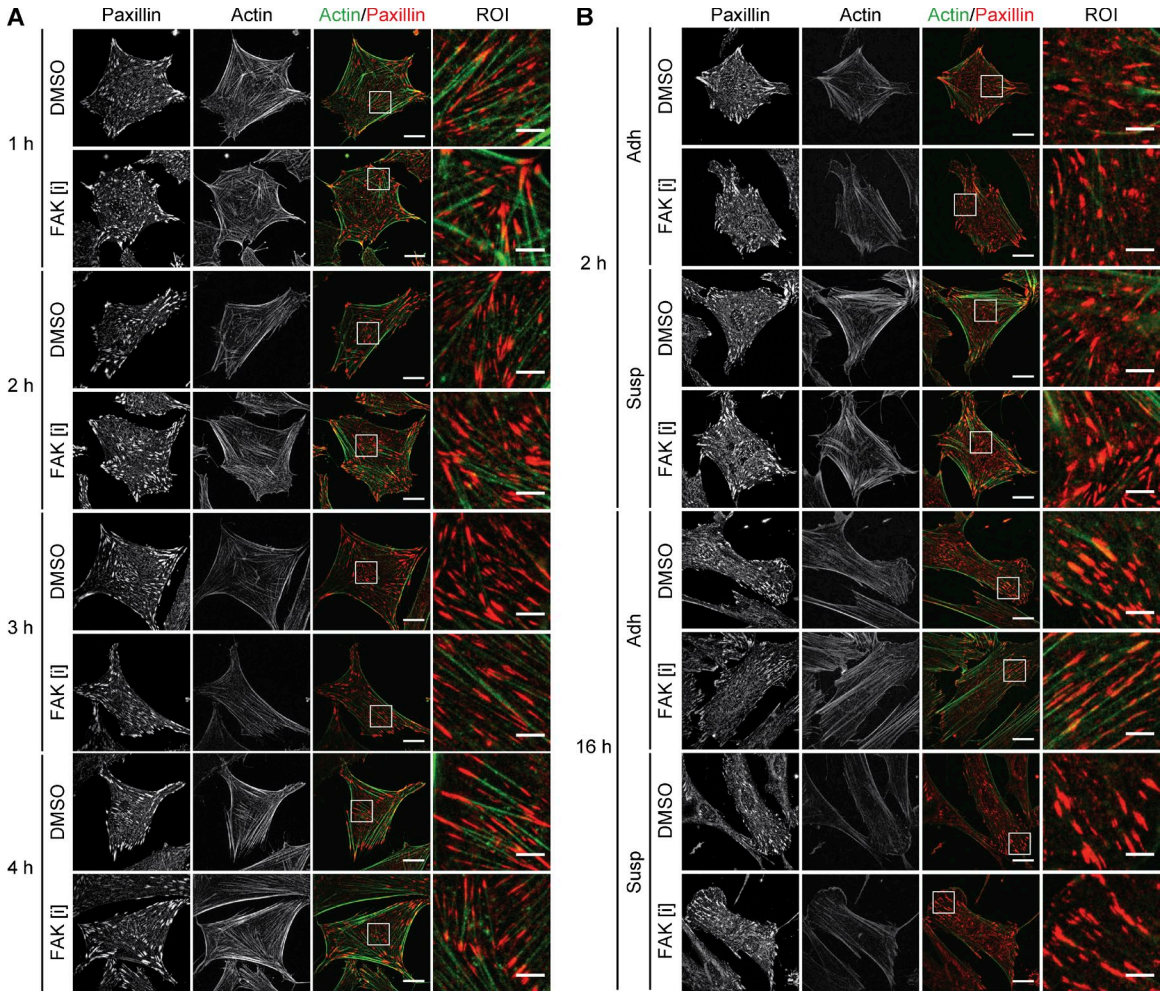

Figure S2. **Effects of the duration of FAK inhibition on paxillin and the actin cytoskeleton.** (A) Immunofluorescence staining of HFF cells spread on FN for 1 h and treated with DMSO or FAK [i] for 1, 2, 3, or 4 h. (B) Immunofluorescence staining of HFF cells treated with FAK [i] added to suspension or prespread cells. To examine effects on cell spreading and IAC formation, DMSO or FAK [i] was added to HFF cells kept in suspension and cells were plated onto FN-coated plates (Susp). To examine effects on IAC maturation, cells kept in suspension were plated onto FN-coated plates for 1 h and treated with DMSO or FAK [i] (Adh). In both cases, cells were fixed after 2 h or 16 h total spreading times. IACs were visualized by staining for paxillin (red) and the actin cytoskeleton was visualized by staining with fluorophore-conjugated phalloidin (green). Bars: (main) 20 µm; (ROI) 5 µm. Representative images are shown.

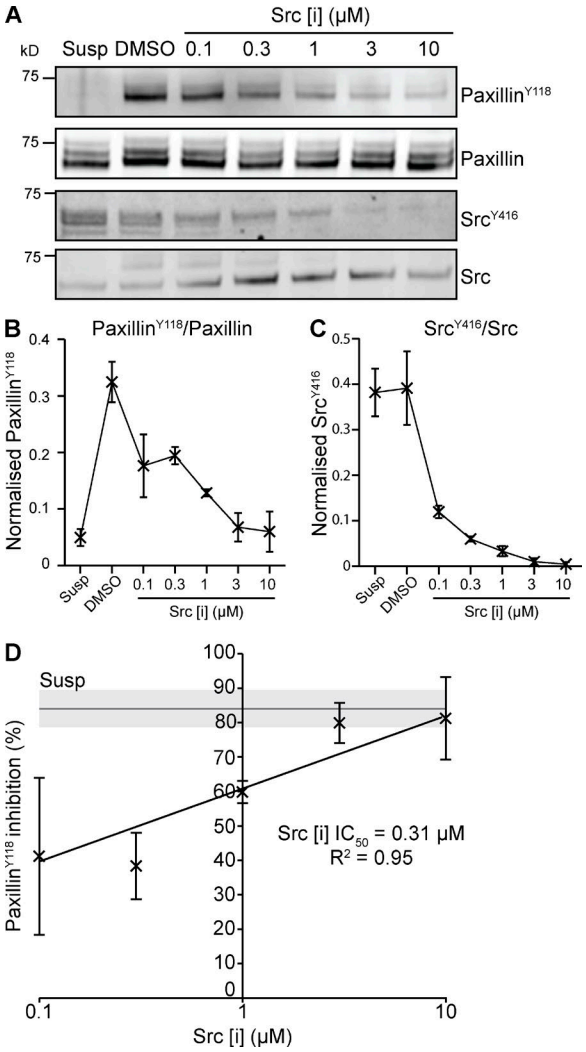

Figure S3. **Inhibition of Src activity by Src [i] in human fibroblasts.** (A) HFF cells spread on FN for 1 h were treated with DMSO or the Src inhibitor AZD0530 (Src [i]) for 1 h using half-log dilutions. Cells kept in suspension for 30 min (Susp) were used to detect adhesion-independent Src activity. Paxillin^{Y118} and Src^{Y416} were used as readouts for Src catalytic activity. Molecular mass values (kD) are displayed. (B and C) Quantification of immunoblotted membranes in A. Phosphorylation values of paxillin^{Y118} (B) and Src^{Y416} (C) were normalized to total protein values of paxillin and Src, respectively, to assess Src catalytic activity (mean ± SEM, $n = 3$). (D) Dose-response curve using paxillin^{Y118} as a readout for Src activity to determine percentage inhibition relative to cells treated with DMSO. Dark gray lines and shading show values for the suspension condition (not used to calculate the trendline, mean ± SEM, $n = 3$). A 50% inhibitory concentration (IC_{50}) was calculated as 0.31 μM Src [i] using the formula $y = 9.19\ln(x) + 60.81$ (y, percentage inhibition; x, Src [i] concentration). Representative images are shown.

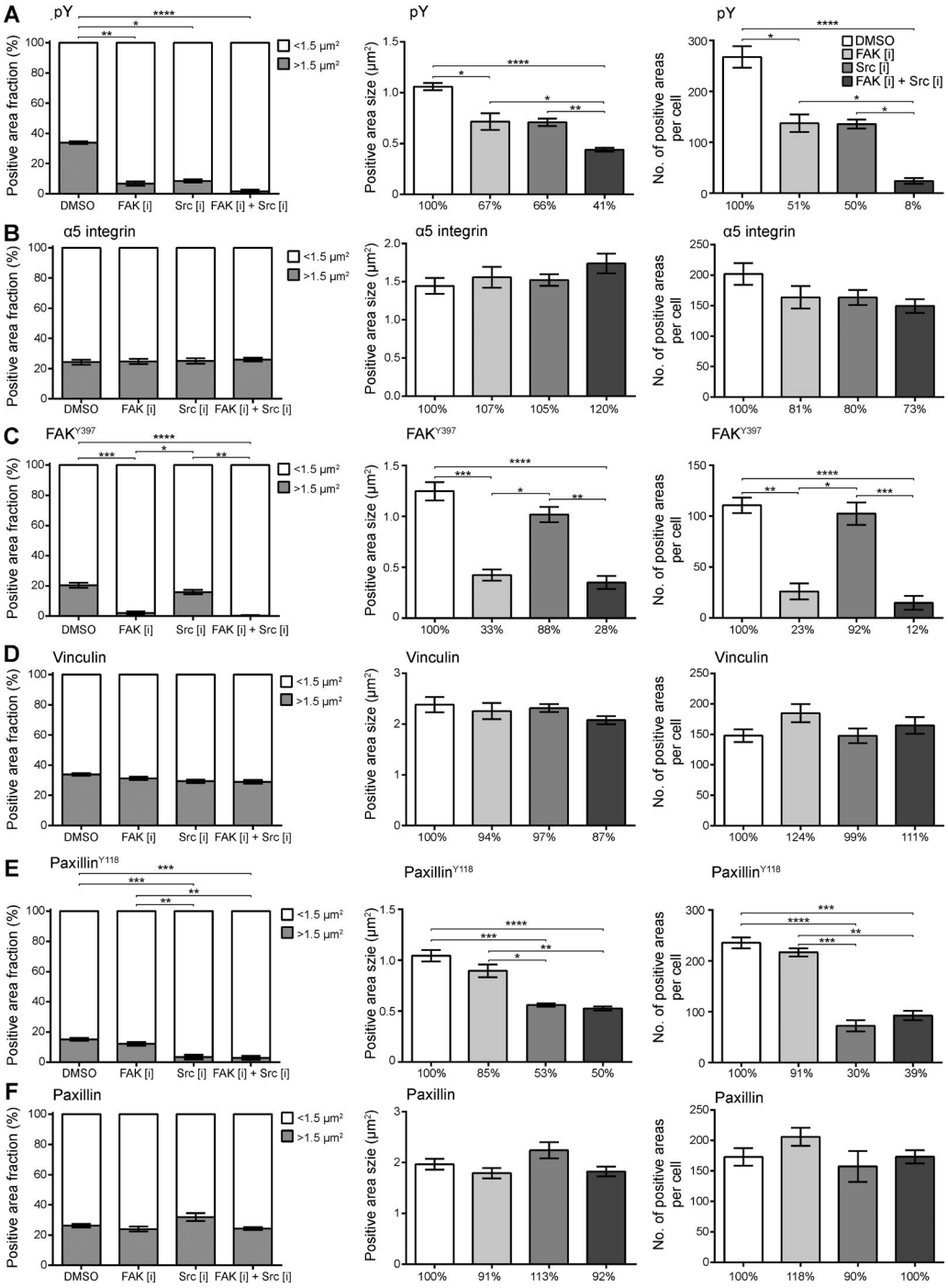

Figure S4. **Additional quantification of the effects of FAK, Src and combined FAK and Src inhibition on IAC proteins and phosphorylation.** (A–F) Additional quantification of images in Fig. 6 for pY (A), α5 integrin (B), FAK^{Y397} (C), vinculin (D), paxillin^{Y118} (E), and paxillin (F). Graphs show quantification of the proportion of positive areas of the indicated protein smaller than or bigger than 1.5 µm^2, the mean positive area size and the number of positive areas measured per cell (mean ± SEM, n = 10 cells). Percentage values relative to the DMSO condition are shown below bars. *, P < 0.05; **, P < 0.01; ***, P < 0.001; ****, P < 0.0001; Kruskal–Wallis test with Dunn's post hoc correction.

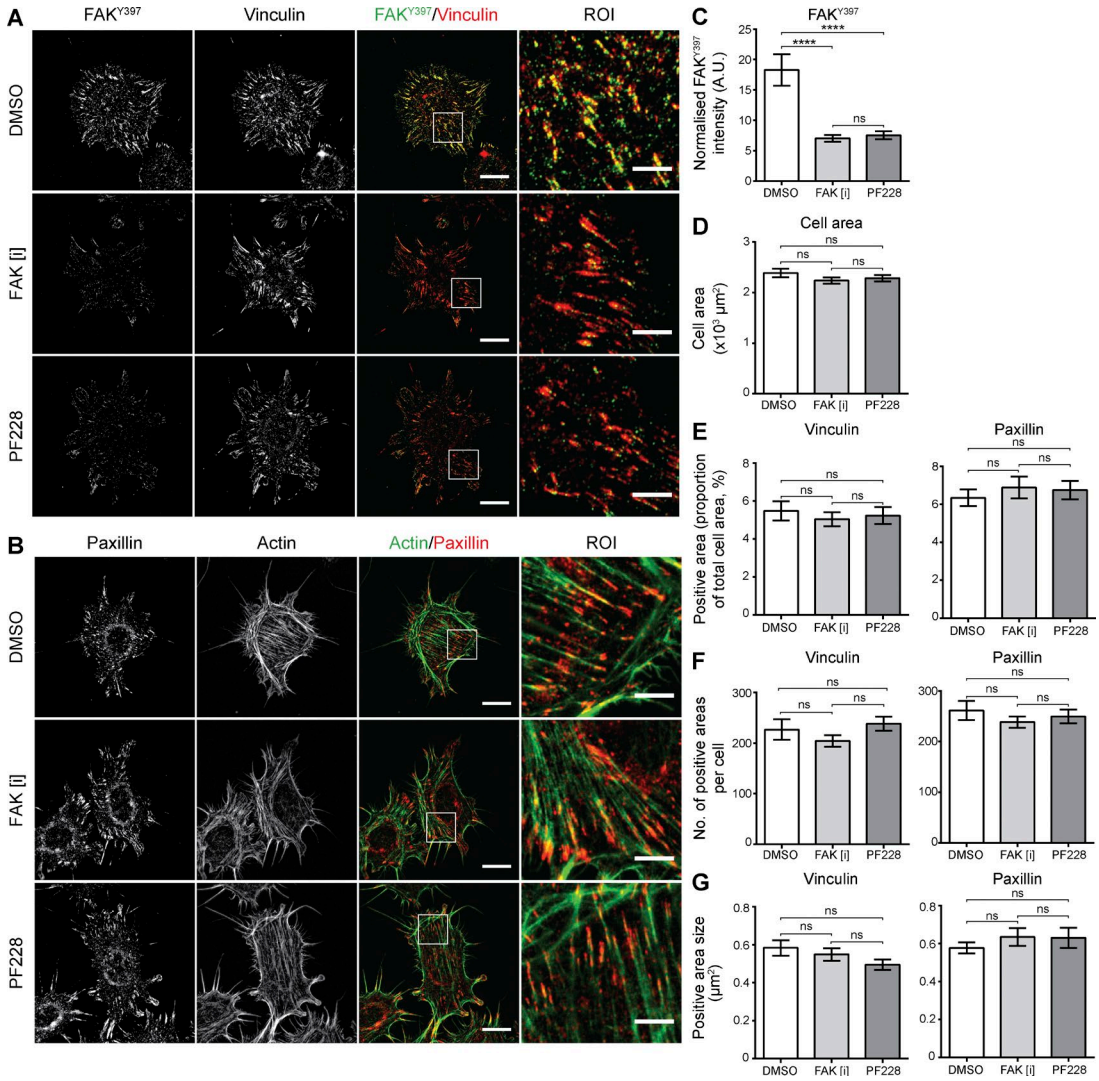

Figure S5. **Inhibition of FAK activity by FAK [i] and PF228 in NIH3T3 cells.** (A and B) NIH3T3 cells spread on FN for 1 h were treated with DMSO, 3 µM FAK [i], or 10 µM PF228 for 1 h. IACs were visualized by staining for FAK^{Y397} (green) and vinculin (red; A) or paxillin (red; B) by immunofluorescence. In B, the actin cytoskeleton was visualized by staining with fluorophore-conjugated phalloidin (green). Bars: (main) 20 µm; (ROI) 5 µm. Representative images are shown. (C–G) Quantification of images in A and B. Graphs show quantification of FAK^{Y397} pixel intensity in vinculin-positive areas (C), the total cell area (D), the proportion of the cell area covered by positive staining of the indicated protein (E), the number of positive areas measured per cell (F), and the mean positive area size (G). In C, FAK^{Y397} intensity values were normalized to the proportion of the cell area covered by vinculin-positive areas. Graphs show mean ± SEM, $n \geq 18$ cells. ****, $P < 0.0001$; ns, not significant; Kruskal–Wallis test with Dunn's post hoc correction. A.U., arbitrary units.

Table S1. **Inhibition of recombinant kinase activity upon treatment with 1 µM FAK [i] or 1 µM PF271**

Kinase[a]	Inhibition[b]	
	1 µM FAK [i]	1 µM PF271
	%	%
AKT2 (h)	0	1.6
AURKB (h)	6.4	–
BTK (h)	7.2	65
CAMKKα (h)	5.2	46
CDK2 CA (h)	38.7	94.4
CHK2 (h)	60	33.1
CK1 (r)	11	0
CK2 (h)	3.5	50.7
CSK (h)	0	29.1
DYRK3 (h)	45.6	66.8
EF2K (h)	18.7	0
EPHB3 (h)	0	41
EPHRA2 (h)	0	29.7
FGFR1 (h)	17.9	80.1
FLT1 (h)	9.8	80
GSK3b (h)	12.3	92.7
HIPK2 (h)	14.6	85.7
IGF1R(h)	49.3	97.6
IKK2 (h)	15.9	12.7
INSR (h)	24.1	57.2
JNK (h)	10.8	7.8
LCK (m)	0	83.8
MAP2K1 (rb)	22.8	77.1
MAPK1 (m)	82.2	88.1
MAPK13 (h)	16.3	42.1
MAPK9 (h)	19.3	12.4
MAPKAKPK5 (h)	6.8	0
MAPKAPK1A (r)	94.8	84.8
MAPKAPK1B (h)	87.7	80.8
MARK3 (h)	23.8	83.5
MELK (h)	0	90.4
MNK1 (h)	0	3.8
MSK1 (h)	15.1	31.9
NEK2a (h)	14.7	4.1
NEK6 (h)	4.7	11.8
P38a (h)	34.3	0
P38b (h)	22.3	7.8
P70S6K (h)	0	26.4
PAK4 (h)	–	88.5
PBK (h)	11	34.5
PDPK1 (h)	14.1	36
PIM3 (h)	0	21.2
PKA (h)	12.2	78.4
PKCa (h)	0	28.4
PKCz (h)	4.1	0
PKD1 (h)	25.3	49
PLK1(h)	69	22.1
PRK2 (h)	7.9	47
ROCK2 (r)	5.1	11.3
SGK (h)	11.1	13.4
Sm MLCK (h)	8.6	16.6
SRPK1 (h)	15.1	33.5
SYK (h)	24.9	91.7
TBK1 (h)	0	73.7
YES (h)	1.3	51.6

h, human; m, mouse; r, rat; rb, rabbit.
[a]FAK [i] was screened against the panel of recombinant enzymes listed.
[b]Percentage of inhibition upon treatment with 1 µM FAK [i] or 1 µM PF271 in a recombinant kinase assay.

Provided online are two Excel tables: Table S2 shows proteins identified in IACs from cells treated with DMSO or FAK [i] by MS and normalized to total protein amount and Table S3 shows proteins identified in IACs from cells treated with DMSO or FAK [i] by MS and normalized to vinculin.

References

Holm, S. 1979. A simple sequentially rejective multiple test procedure. *Scand. J. Stat.* 6:65–70.

Horton, E.R., A. Byron, J.A. Askari, D.H.J. Ng, A. Millon-Frémillon, J. Robertson, E.J. Koper, N.R. Paul, S. Warwood, D. Knight, et al. 2015. Definition of a consensus integrin adhesome and its dynamics during adhesion complex assembly and disassembly. *Nat. Cell Biol.* 17:1577–1587. http://dx.doi.org/10.1038/ncb3257

Mitchell, A., H.Y. Chang, L. Daugherty, M. Fraser, S. Hunter, R. Lopez, C. McAnulla, C. McMenamin, G. Nuka, S. Pesseat, et al. 2015. The InterPro protein families database: the classification resource after 15 years. *Nucleic Acids Res.* 43:D213–D221. http://dx.doi.org/10.1093/nar/gku1243

Winograd-Katz, S.E., R. Fässler, B. Geiger, and K.R. Legate. 2014. The integrin adhesome: from genes and proteins to human disease. *Nat. Rev. Mol. Cell Biol.* 15:273–288. http://dx.doi.org/10.1038/nrm3769